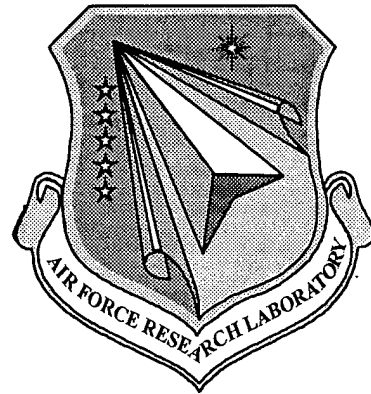


AFRL-MN-EG-TR-2000-7006

Radarometer Sensor -- Simultaneous Active and Passive Imaging Using a Common Antenna

Darryl G. Huddleston
Captain James C. Savage
Bryce M. Sundstrom
Byron W. Belcher
Air Force Research Laboratory, Munitions Directorate
Advanced Guidance Division
Seeker Branch (AFRL/MNGS)
101 W. Eglin Blvd
Eglin AFB FL 32542 - 6810



Doc Ewen
Millitech Corporation
20 Industrial Drive East
Post Office Box 109
South Deerfield MA 01373-0109

CONTRACT NO. FO8630-98-C-0045

MAY 1999

FINAL REPORT FOR PERIOD MARCH 1998 - JANUARY 1999

Approved for public release; distribution is unlimited.

20000228 098

AIR FORCE RESEARCH LABORATORY, MUNITIONS DIRECTORATE

Air Force Materiel Command ■ United States Air Force ■ Eglin Air Force Base


THIS QUALITY INSPECTED 3


NOTICE

When Government drawings, specifications, or other data are used for any purpose other than in connection with a definitely Government-related procurement, the United States Government incurs no responsibility or any obligation whatsoever. The fact that the Government may have formulated or in any way supplied the said drawings, specifications, or other data, is not to be regarded by implication, or otherwise in any manner construed, as licensing the holder, or any other person or corporation; or as conveying any rights or permission to manufacture, use, or sell any patented invention that may in any way be related thereto.

This technical report is releasable to the National Technical Information Services (NTIS). At NTIS it will be available to the general public, including foreign nations.

This technical report has been reviewed and is approved for publication.


MARTIN F. WEHLING
Technical Director
Advanced Guidance Division


DARRYL G. HUDDLESTON
Program Manager

If your address has changed, if you wish to be removed from our mailing list, or if your organization no longer employs the addressee, please notify AFRL/MNG, Eglin AFB FL 32542-6810, to help us maintain a current mailing list.

Do not return copies of this report unless contractual obligations or notice on a specific document requires that it be returned.

REPORT DOCUMENTATION PAGE

Form Approved
OMB No. 0704-0188

Public reporting burden for this collection of information is estimated to average 1 hour per response, including the time for reviewing instructions, searching existing data sources, gathering and maintaining the data needed, and completing and reviewing the collection of information. Send comments regarding this burden estimate or any other aspect of this collection of information, including suggestions for reducing this burden, to Washington Headquarters Services, Directorate for Information Operations and Reports, 1215 Jefferson Davis Highway, Suite 1204, Arlington, VA 22202-4302, and to the Office of Management and Budget, Paperwork Reduction Project (0704-0188), Washington, DC 20503.

1. AGENCY USE ONLY (Leave blank)		2. REPORT DATE MAY 1999		3. REPORT TYPE AND DATES COVERED FINAL March 1998 - January 1999	
4. TITLE AND SUBTITLE Radarometer Sensor - Simultaneous Active and Passive Imaging Using a Common Antenna				5. FUNDING NUMBERS Contract #: F08630-98-C-0045 JON: 30058132 PE: 65502F PR: 3005 TA: 81 WU: 32	
6. AUTHOR(S) (AFRL/MNGS) Darryl G. Huddleston, Captain James C. Savage, Bryce M. Sundstrom, and Byron W. Belcher; (Millitech) Doc Ewen					
7. PERFORMING ORGANIZATION NAME(S) AND ADDRESS(ES) Millitech Corporation 20 Industrial Drive East Post Office Box 109 South Deerfield MA 01373-0109				8. PERFORMING ORGANIZATION REPORT NUMBER	
9. SPONSORING/MONITORING AGENCY NAME(S) AND ADDRESS(ES) (Program Mgr Name & Ph #) Air Force Research Laboratory, Munitions Directorate Advanced Guidance Division Seeker Branch (AFRL/MNGS) 101 W. Eglin Blvd Eglin AFB FL 32542 - 6810 Program Manager: Darryl Huddleston, AFRL/MNGS, (850) 882-5607				10. SPONSORING/MONITORING AGENCY REPORT NUMBER AFRL-MN-EG-TR-2000-7006	
11. SUPPLEMENTARY NOTES Availability of this report is specified on the verso of front cover.					
12a. DISTRIBUTION/AVAILABILITY STATEMENT Approved for Public Release; Distribution is Unlimited				12b. DISTRIBUTION CODE	
13. ABSTRACT: Report Developed Under SBIR Contract. The ability to obtain simultaneous active and passive millimeter wave images using a common antenna has numerous DOD as well as commercial applications. Radiometric and radar images are not new, nor are simultaneous passive and active images of a common scene. The feature, which is unique to the radarometer concept, is simultaneous use of the same antenna by a radar and a radiometer, operating in the same frequency band at a nominal pixel scanning rate of 1,000 per second. The radarometer sensor is capable of operating in both the passive and active modes either individually, in time sequence, or simultaneously. The radarometer uses a common high-speed mechanically scanned antenna aperture capable of generating active and passive millimeter wave images simultaneously. The important feature of the radarometer design that allows simultaneous active and passive operation is the use of an RF diplexer which separates the signals associated with the radar and radiometer modes. The typical frequency separation displacement is 5 GHz, at a nominal operating frequency of 95 GHz. The results of measurements performed on an engineering test unit will be described.					
14. SUBJECT TERM SBIR Report, passive, active, millimeter wave, radiometer, radar, data fusion				15. NUMBER OF PAGES 23	
17. SECURITY CLASSIFICATION OF REPORT UNCLASSIFIED				18. SECURITY CLASSIFICATION OF THIS PAGE UNCLASSIFIED	
19. SECURITY CLASSIFICATION OF ABSTRACT UNCLASSIFIED		20. LIMITATION OF ABSTRACT SAR			

PREFACE

This program was conducted by Millitech Corporation, 20 Industrial Drive East, PO Box 109, South Deerfield MA 01373, under CONTRACT F08630-98-0045 with AFRL/MNGS, Eglin Air Force Base FL 32542-6810. Darryl Huddleston, Program Manager, and AFRL/MNGS managed the program for the Air Force Munitions Directorate. The program was conducted during the period from March 24, 1998 and November 24, 1998.

The author wishes to acknowledge the technical assistance of the Eglin Air Force Base STAG team; specifically, Darryl Huddleston, Bryce Sundstrom, Roger Smith, Capt. James Savage, and Byron Belcher.

TABLE OF CONTENTS

<u>Section</u>	<u>Title</u>	<u>Page</u>
I	INTRODUCTION	1
II	TECHNICAL OBJECTIVES	1
III	VERIFICATION OF CONCEPT	1
IV	DEMONSTRATION OF SIMULTANEOUS ACTIVE AND PASSIVE IMAGING	9
V	CONCLUSIONS AND RECOMMENDATIONS	13

LIST OF FIGURES

<u>Figure</u>		<u>Page</u>
1	Breadboard Radarometer Operating Frequencies	2
2	Prototype Radarometer Diplexer Performance	2
3	Prototype Radarometer Diplexer Performance	3
4	Photograph of Diplexer in Test Setup #1	3
5	Photograph of Diplexer and Isolator in Test Setup #1	4
6	Verification of Radarometer Concept, Test Setup #1	5
7	Photograph of Test Setup #1	5
8	Calibration, Paddle Wheel, (T_{AMB-LN}), 5 mv Scale	7
9	Calibration, Paddle Wheel, (LN Cycle), 2 mv Scale	8
10	Verification of the Radarometer Concept	8
11	Demonstration of Radarometer Mode – Test Setup #2	10
12	Some Challenges Associated with Test Setup #2	11
13	Radarometer Breadboard Demonstration	12
14	Passive Image, from the Millitech Tower, ROSCAM A14B	13

LIST OF TABLES

<u>Table</u>		<u>Page</u>
1	Test Setup for Verification of Radarometer Concept	6
2	Strip Chart Data Records	7

LIST OF ABBREVIATIONS AND ACRONYMS

ΔK	Delta Degrees Kelvin
CW	Continuous Wave
EMI	Electro-Magnetic Interference
ETU	Engineering Test Unit
FOV	Field of View
LO	Local Oscillator
LN	Liquid Nitrogen
prf	Pulse Repetition Frequency
Radarometer	Simultaneous Radar-Radiometer Imaging Mode
RAM	Radar Absorbing Material
ROSCAM	Radiometric One Second Camera
S/N	Signal-to-Noise ratio
STAGCAM	Smart Tactical Autonomous Guidance Camera
T_{AMB}	Temperature of the Ambient Load
T_{LN}	Temperature of Liquid Nitrogen
X/R	Transmitter and Receiver

(This page intentionally blank.)

I. INTRODUCTION

The ability to obtain simultaneous active and passive millimeter wave images using a common antenna (Radarometer Concept) has numerous DoD as well as commercial applications. Radiometric and radar images are not new, nor are simultaneous passive and active images of a common scene. *The feature that is unique to the Radarometer Concept is simultaneous use of the same antenna by a radar and a radiometer, operating in the same frequency band at a nominal pixel scanning rate of 1,000 per second.* The radarometer sensor is capable of operating in both the passive and active modes either individually, in time sequence, or simultaneously. The radarometer uses a common high-speed mechanically scanned antenna aperture capable of generating active and passive millimeter wave images simultaneously.

The important feature of the radarometer design that allows simultaneous active and passive operation is the use of a RF diplexer which separates the signals associated with the radar and radiometer modes. The typical frequency separation displacement is 5 GHz, at a nominal operating frequency of 95 GHz. The results of measurements performed on an engineering test unit will be described.

The goal of this SBIR Phase I effort was the design, assembly and demonstration of a practical millimeter wave camera capable of obtaining simultaneous passive and active airborne images during adverse weather conditions that preclude the use of either optical or infrared imaging cameras. The proposed approach was based on use of an existing radiometric receiver and a high-speed mechanical antenna scanning mechanism in a configuration unique to the airborne imaging scenario.

II. TECHNICAL OBJECTIVES

Three objectives were accomplished:

- Verification of simultaneous radiometer and radar on a non-interfering basis when using a common antenna (Radarometer Concept)
- Demonstration of simultaneous active and passive imaging in the radarometer mode
- Design, assemble, and test a radarometer Engineering Model

III. VERIFICATION OF CONCEPT

Verification of the radarometer concept required a test configuration capable of determining through measurement the performance characteristics of a radar operating simultaneously with a radiometer, when sharing a common antenna. *A key feature of the test configuration was the ability to measure any variations in radiometer sensitivity when the power level, prf and pulse width of the radar were at operational values.* Reasonable power level, prf, and pulse widths were based on nominal airborne operational requirements.

Two critical components made the radarometer mode possible. The components were a RF diplexer and isolator. The diplexer separates the radar and radiometer signals at the output of the

scanning antenna system. We are indebted to Dr. Sridhar Kanamaluru for the design of the frequency diplexer, and Dr. Neal Erickson for the design of the isolator. The isolator provides a low-loss broadband match for the radiometer, when connected to the diplexer. The breadboard radar and radiometer operating frequencies are shown in Figure 1.

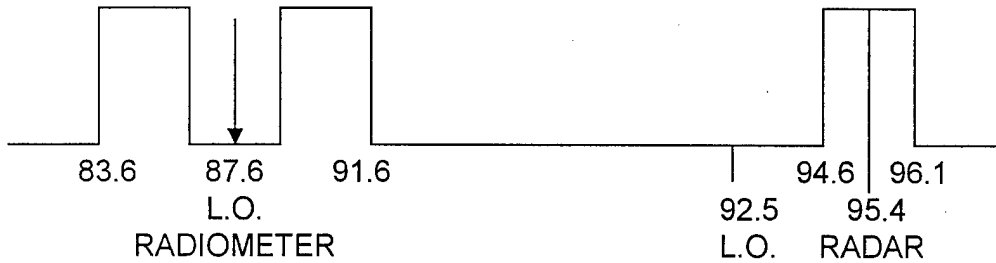


Figure 1. Breadboard Radarometer Operating Frequencies

The measured performance of the prototype diplexer is shown in Figures 2 and 3. The loss in the radiometer channel was higher than anticipated. Performance of the prototype was more than adequate to verify the efficacy of the radarometer concept. A photograph of the diplexer and isolator, integrated into the radarometer Test Setup #1, is shown in Figures 4 and 5.

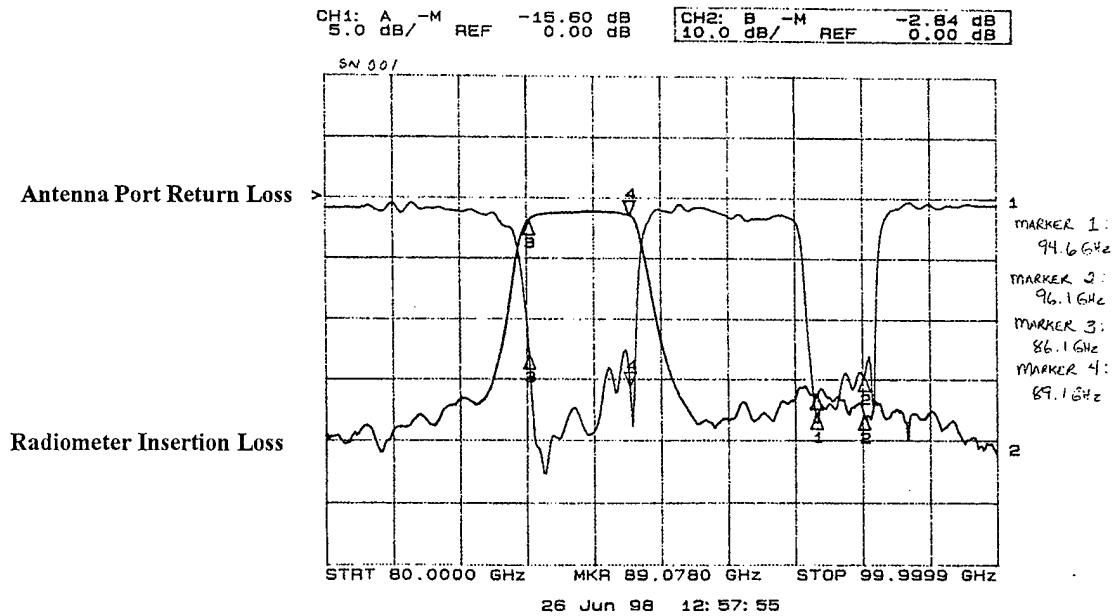


Figure 2. Prototype Radarometer Diplexer Performance (Radiometer Insertion)

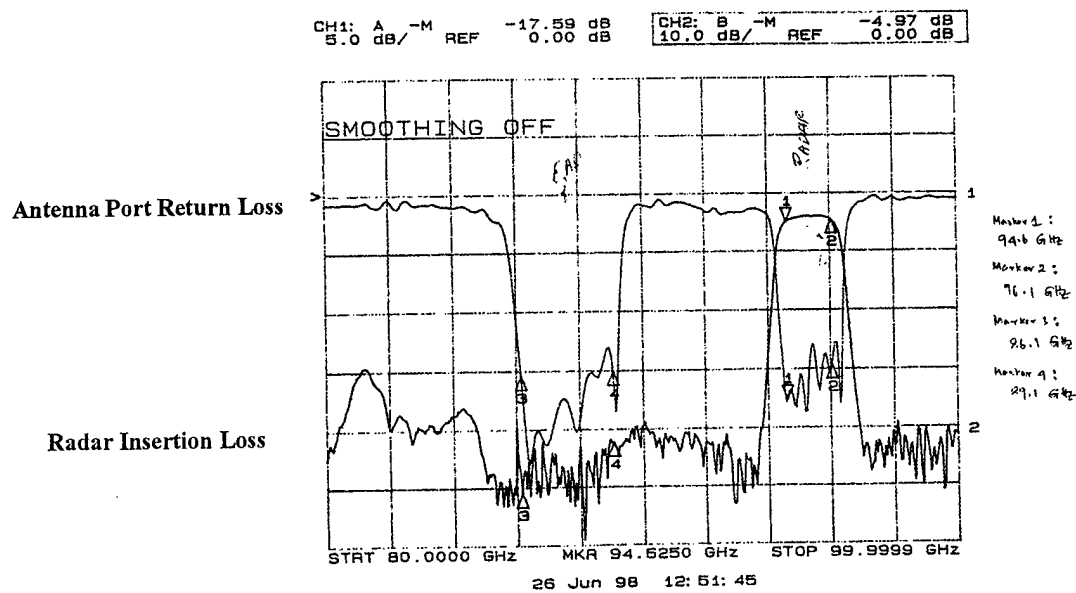


Figure 3. Prototype Radarometer Diplexer Performance (Radar Insertion)

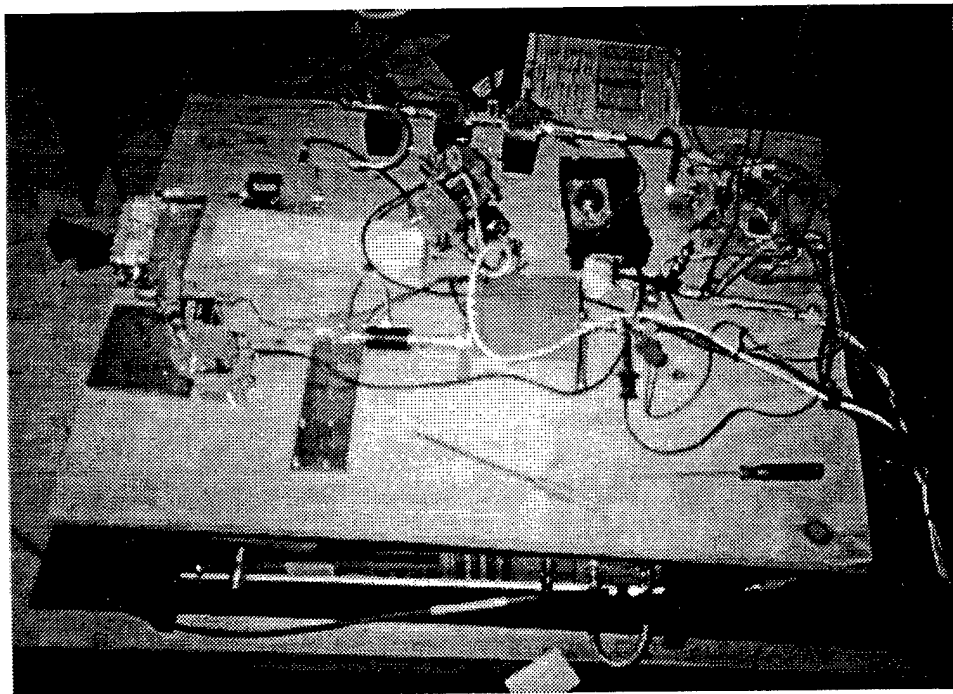


Figure 4. Photograph of Diplexer in Test Setup #1

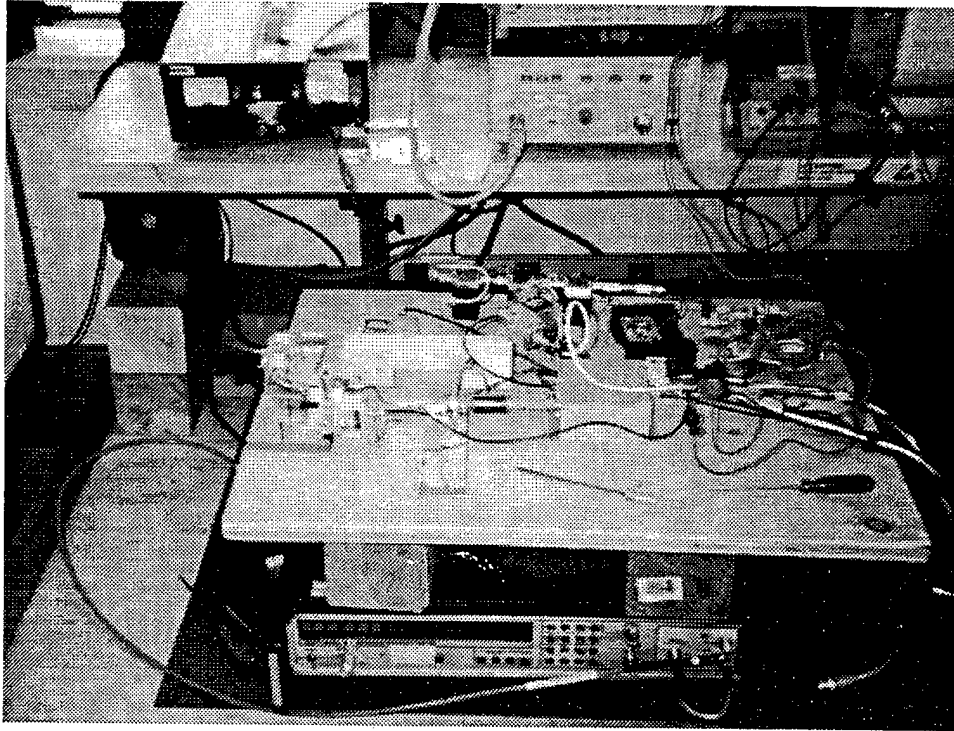


Figure 5. Photograph of Diplexer and Isolator in Test Setup #1

The test setup used for verification of the radarometer concept is shown in Figure 6. Note that:

- To prove the concept, isolation between the radar and radiometer signals through the common feed is adequate. An imaging mode is not required.
- A STAGCAM radiometric receiver (an extremely sensitive laboratory radiometer specifically designed to acquire phenomenology data) was used as the radiometer in the radarometer test configuration.
- Adjustment of radar parameter values was confined to prf, pulse width and transmitter power.
- The transmitter power was set at the level needed to achieve a 20 dB S/N from natural terrain when observed at an altitude of 400 meters.
- The radiometric input signal to the common antenna feed was broadband noise, square-wave modulated between the two effective brightness temperature levels of ambient and liquid nitrogen.
- The input signal was derived by rotating a paddle wheel, with Radar Absorbing Material (RAM) on the propellers, in front of RAM immersed in liquid nitrogen in a Styrofoam container.
- The temperature-modulated input signal varies in a near square wave fashion between the nominal extremes of 80K and 300K, and provides a measure of the radiometer Y-factor, effective noise figure, and sensitivity. In addition, it provides a direct radiometric measurement of any degradation in radiometer performance associated with the simultaneous operation of the radar, or the adjustment of its operating parameters.

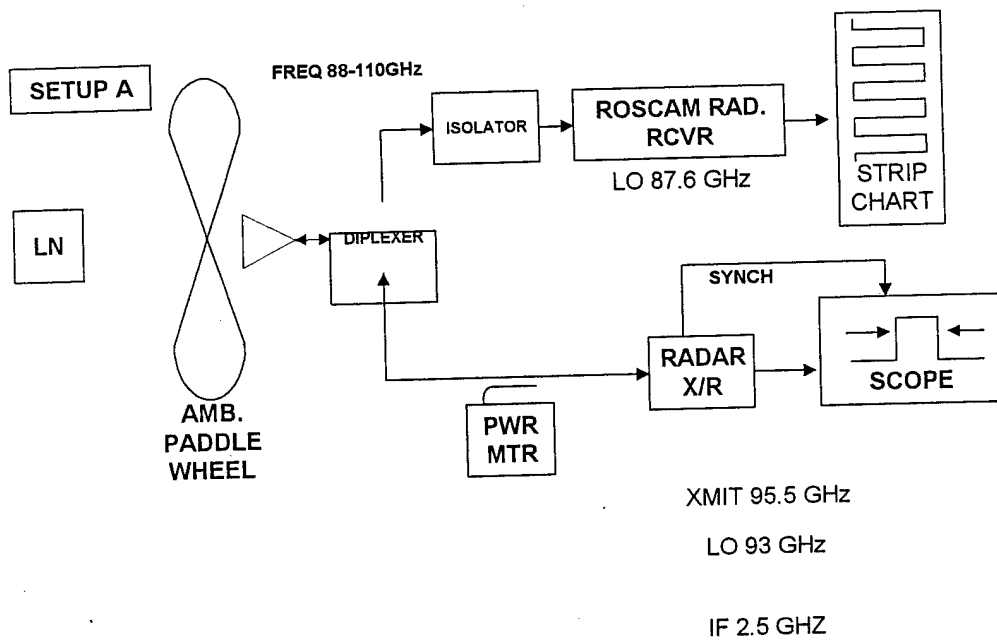


Figure 6. Verification of Radarometer Concept, Test Setup #1

A photograph of Test Setup #1 is shown in Figure 7. The radiometer and radar parameter values used in Test Setup #1 are listed in Table 1.

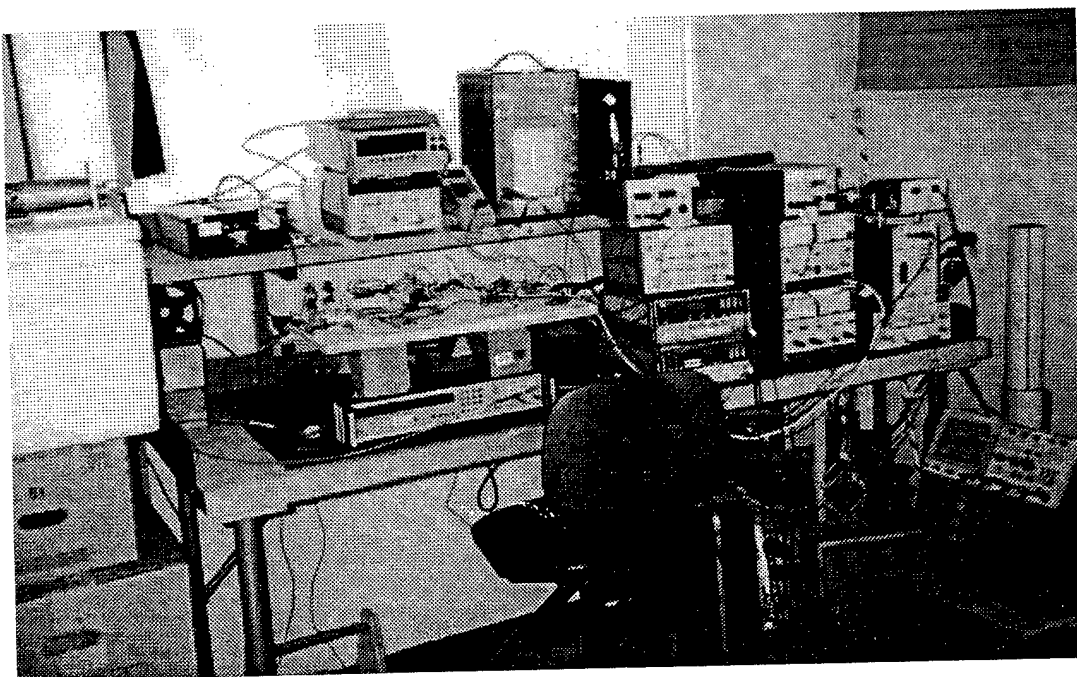


Figure 7. Photograph of Test Setup #1

Table 1. Test Setup for Verification of Radarometer Concept

Parameter	Determined by	Nominal Value
RADIOMETER MODE		
LO Frequency	Band Pass of Diplexer	87.6 ±1.5 GHz
IF Bandwidth	Band Pass of Diplexer	0.1 – 1.5 GHz
Noise Temperature	Diplexer and Isolator Loss, plus receiver noise	2000 K
Integration Time	Pixel Sample Time	0.5 ms
Mode	Superheterodyne “Total Power”	Dual Side Band
Sensitivity	Statistical Noise Fluctuation Level	2 K _{rms}
Transmitter Frequency	Band Pass of Diplexer	95.4 ± 0.75 GHz
RADAR MODE		
Pulse Duration	Minimum Alt. (200 m) Roundtrip time (1.33μs)	1 μs
prf	Maximum Alt. (400 m) Roundtrip time (2.67 μs)	400 KHz
Duty factor	Pulse width times prf	0.4
Transmitter power	Measurement results ¹	40 mW Peak
S/N (Avg.)	Measurement results ¹	≥ 20 dB

The measurement procedure followed the sequence:

- Radar off
- Radar operating in a Continuous Wave (CW) mode at the operational power level
- Radar operating in the modulation mode
- Radar operating in the CW mode
- Radar off

The strip chart data records obtained during the Verification of Concept test series are listed in Table 2. Copies of the data records are included as Figures 8, 9, and 10. All data records were obtained at the radiometer output, to verify that simultaneous operation of the radar does not contaminate radiometer performance.

Table 2. Strip Chart Data Records

Figure #	Description
8	Calibration, paddle wheel, (T _{AMB} -LN) on 5 mV scale
9	Calibration, paddle wheel (LN cycle) on 2 mV scale
10	Radar off – Radiometer (LN cycle) on 2 mV scale Radar on – CW Radiometer (LN cycle) on 2 mV scale Radar on – Modulated. Radiometer (LN cycle) on 2 mV scale Radar on – CW Radiometer (LN cycle) on 2 mV scale Radar off – Radiometer (LN cycle) on 2 mV scale

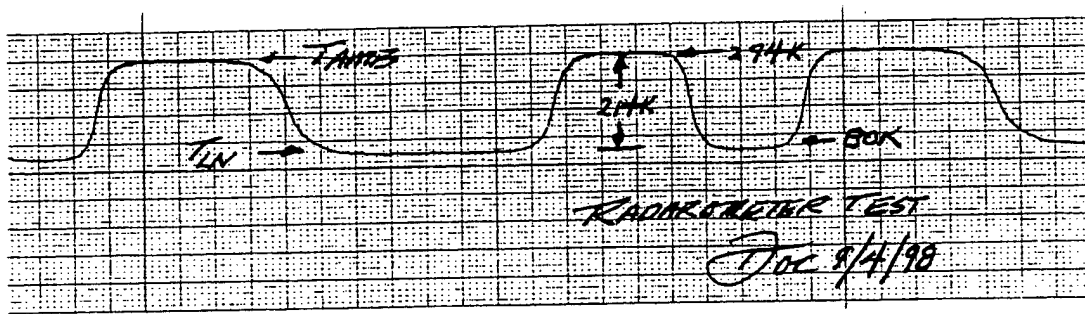


Figure 8. Calibration, Paddle Wheel, (T_{AMB}-LN), 5 mV Scale

To obtain calibration data, the two-bladed, RAM coated, paddle wheel was rotated slowly in front of RAM immersed in liquid nitrogen. The radiometer channel saw a modulated noise input signal, T_{AMB}, when it viewed the paddle blade and saw the liquid nitrogen RAM, T_{LN}, when the paddle blade was not present. The lack of “square wave” symmetry was due to the slow rotation rate of the wheel and the tendency of the wheel shaft to stick during part of the cycle. This data is shown in Figure 8. The calibration was found by:

$$\text{Calibration} = \frac{\Delta K}{\Delta \text{ chart division}} = \frac{214}{17} = 12.6\text{K/division}$$

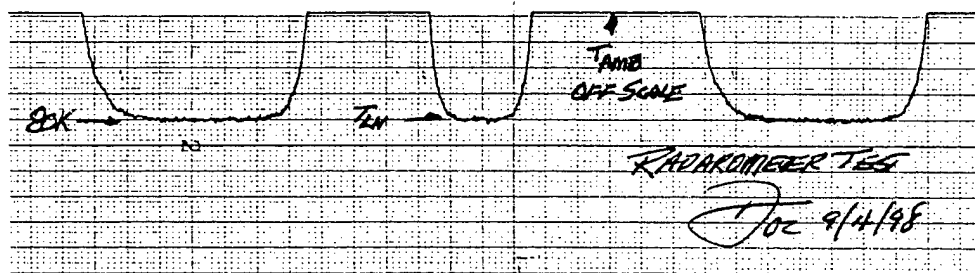


Figure 9. Calibration, Paddle Wheel (LN cycle), 2 mV Scale

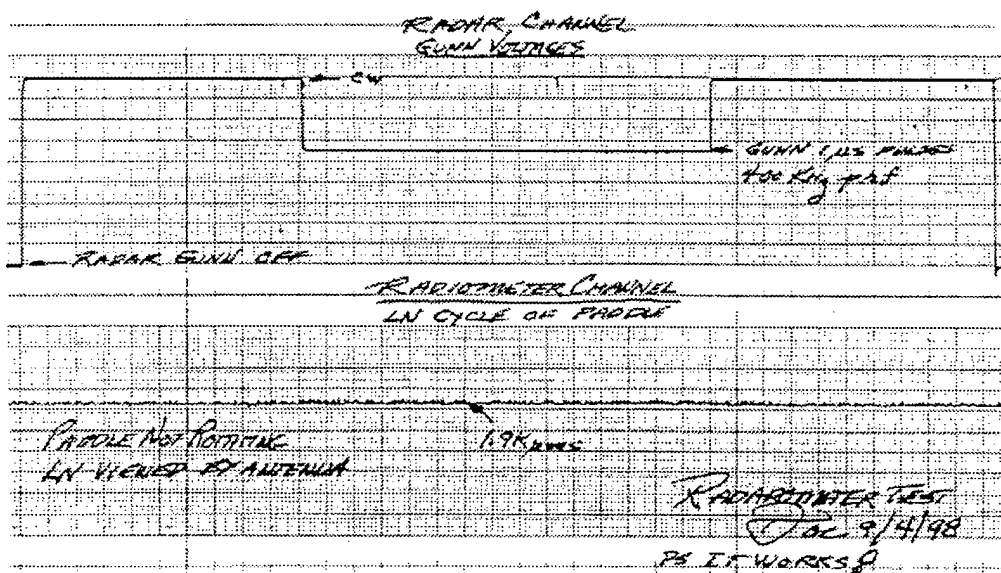


Figure 10. Verification of Radarometer Concept

In Figure 9, the data scale was expanded to show only the LN half cycle. This allowed the noise fluctuations to be more easily detected. The scale was also changed to 2 mV full scale producing a scale factor of $5/2 = 2.5$. The calibration was then found to be $12.6/2.5 = 5K/\text{division}$. The paddle wheel rotation was then stopped on the LN half cycle such that the radarometer feed continuously observed RAM immersed in LN. The output of the radiometer channel, shown in the lower diagram of Figure 10, was continuously recorded throughout the remainder of the test. Any change in the output signal would indicate interference with the performance of the radiometer channel. A 95% peak-to-peak value of 1.5 divisions was found from the Figure 10 lower diagram. With each chart division equal to 5K, this peak-to-peak level was calculated to be 7.5K. Since the 95% peak-to-peak fluctuation level of Gaussian noise is approximately four times the rms value, a value of 1.9K rms was determined. This value represents the minimum detectable signal level for interference between the radar and radiometer channels.

The radar Gunn parameters were adjusted to 40 mW CW, 1 μ s pulse width and 400 KHz prf. The Gunn transmitter frequency was set to the center of the radar channel and the Gunn driver voltages were recorded. The test sequence was then conducted. The radar channel Gunn voltages are shown in the upper diagram of Figure 10. The Gunn off, CW on, modulation on, CW on, and Gunn off regions are shown on the strip chart recording. Inspection of the data records indicates that no detectable degradation of the radiometer performance was associated with the operation of the radar. *The ability to operate simultaneously in a radar and radiometer mode, when sharing a common antenna was demonstrated by the results of this test.*

IV. DEMONSTRATION OF SIMULTANEOUS ACTIVE AND PASSIVE IMAGING

An important step in our test series was confirmation of the split screen software performance. The split screen presentation provides a simultaneous radiometric and radar view of a target scenario. Initially, we felt that the geometry of the test setup, when located in the Millitech tower, would preclude the possibility of obtaining images in either the active or passive mode, to adequately demonstrate radarometer capabilities.

The test scenario, as viewed from the tower, provides a view over a metal roof in the foreground, with trees in the immediate background. One large pine provides a unique feature in the background.

The view over the metal roof complicates the efficacy of sky noise reflecting plates when used against a metal background. It also eliminates the possibility of using automobiles or similar targets as the central focus of a radiometric image. The radiometric image for the tower scenario shows the background foliage line against the sky background and the reflection of the emitted radiation from the foliage as it bounces off the metal roof. The background radiometric target is black body radiation from the foliage. There is no reflected sky noise associated with the foliage. However, the sky noise does present a cold background for the skyline profile of the foliage. An easily identified background target is the tall pine located well beyond the far edge of the rooftop. The noise radiated by the tall pine is easily identified with its reflection off the top of the roof.

The target scenario for the radar was more controllable, in the sense that we were able to locate corner reflectors on tripods placed on top of the roof. However, this did not eliminate the appearance of the reflected image of the corner reflectors seen at the appropriate bounce angle off the metal roof. There were other distractions that initially discouraged our attempt to demonstrate simultaneous radar and radiometer operation using a common antenna.

One reasonable alternative was to operate the radar channel in a radiometer mode and display radiometer images obtained simultaneously at 87 and 95 GHz. This was viewed as less attractive than a demonstration of the normal radar/radiometer mode. A functional block diagram of Test Setup #2, used for the demonstration of the radarometer mode is shown in Figure 11.

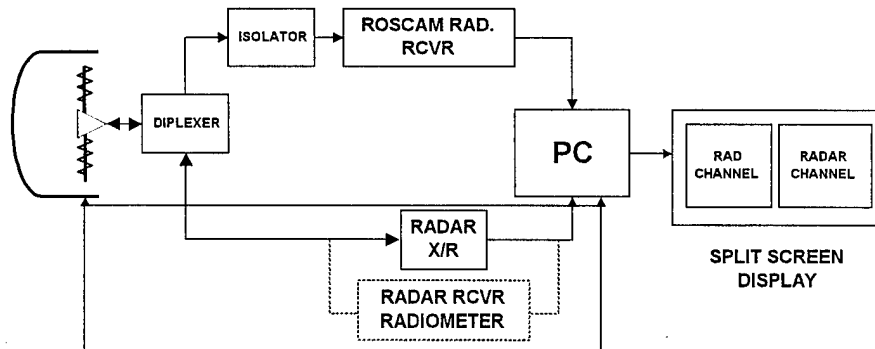


Figure 11. Demonstration of Radarometer Mode – Test Setup #2

A collage of photos taken of the test setup and test site is included as Figure 12. Some of the challenges associated with this test setup included:

Upper left

- Air conditioning units on the metal roof
- Step ladder
- Power and control cable to the Tower roof
- Rope to the Tower roof
- Stand pipes passing through the Tower roof in the background

Upper right

- Tall pine tree in the background
- Two radar corner reflectors supported on tripods on the roof

Lower right

- Step ladder for access to the rooftop
- Open window used for access to the roof
- Radarometer Engineering Test Unit (ETU)

Lower left

- The ETU showing test equipment as well as functional parts of the radarometer
- ETU Cable harness that was particularly susceptible to EMI (Electro-Magnetic Interference)

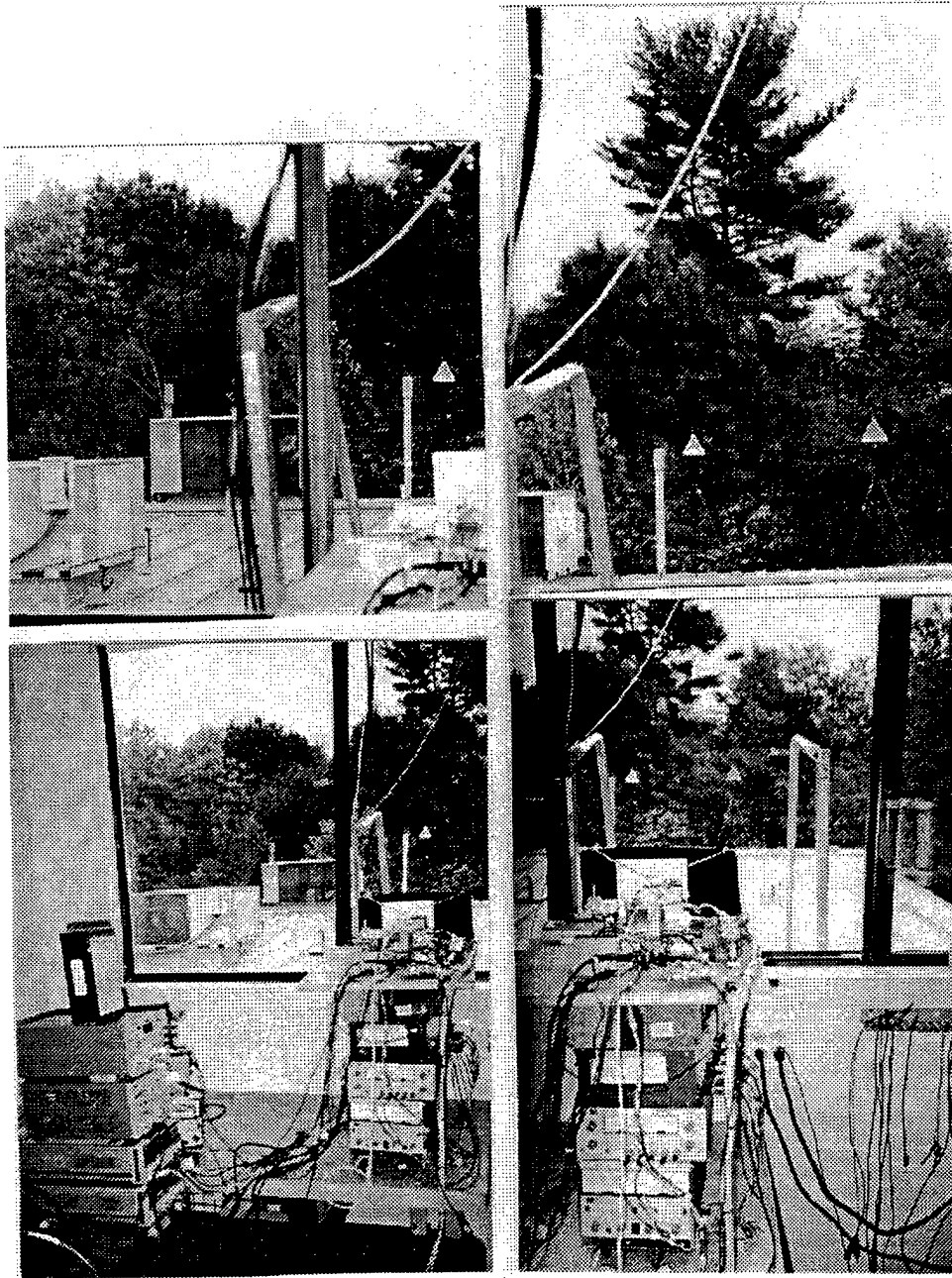
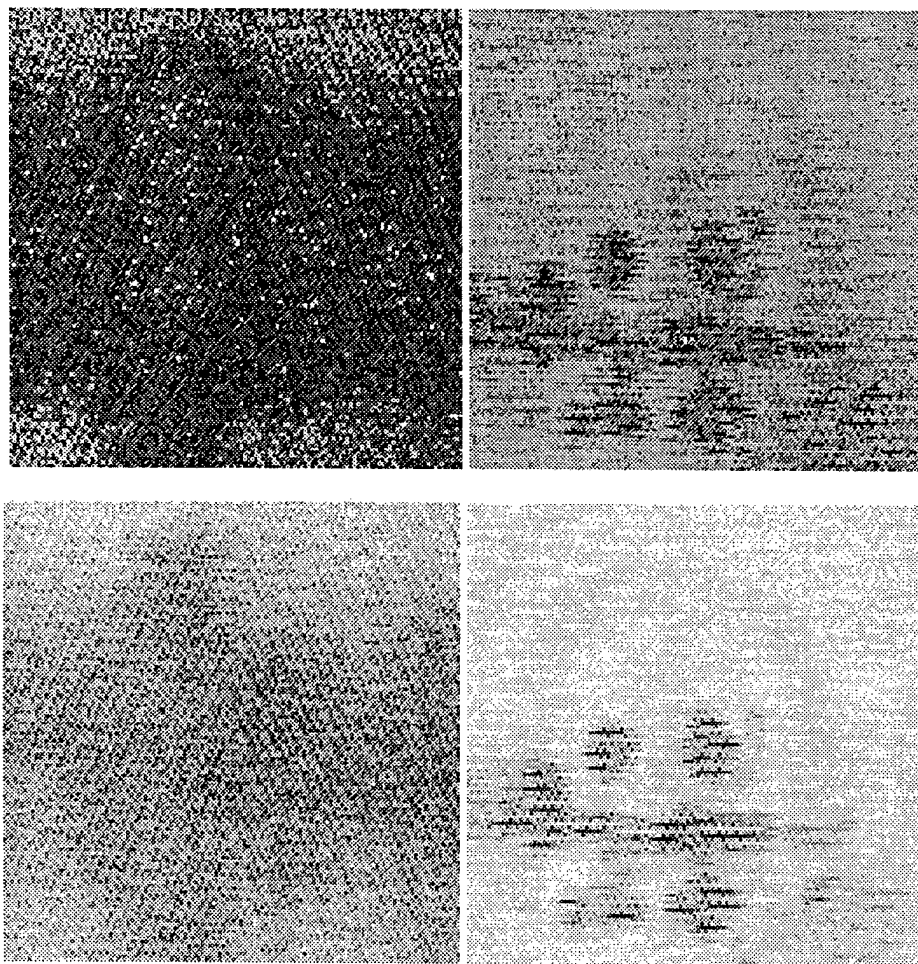


Figure 12. Some Challenges Associated with Test Setup #2

Despite the shortcomings of the test site, we successfully demonstrated the radarometer mode. Hard copies of the PC display, when viewing the scene as observed from the Millitech Tower, are shown in Figure 13. Both color and black and white versions are included. The radiometer channel clearly shows the tall pine and its reflection off the roof.

The radar image shows the two corner reflectors viewed directly by the radar, as well as the two bounce signals lower in the image scan. The edge of the roof is easily identified between the two images of each corner reflector. The air conditioning unit is seen to the left, on the edge of the roof.



Radiometer Channel
88 GHz

FOV
32° x 32°

Radar Channel
95 GHz

Figure 13. Radarometer Breadboard Demonstration

Both radiometer images show a striation running through the image, which is typical of EMI. It is evident from Figure 13 that EMI is controlling the sensitivity threshold level for the radiometer images. The effect of the radar is negligible.

To verify that the radiometer image was contaminated by EMI, we took a picture of the scene with a *Radiometric One Second Camera (ROSCAM)*, which had undergone a significant EMI reduction program. ROSCAM is designed to take a two-dimensional, passive, millimeter wave image at a 1 Hz rate. During the earlier helicopter flights, the ROSCAM was incapable of flying over the ridge of the Mt. Holyoke Range without experiencing radar EMI from Westover Air Force Base and UHF TV interference from Hartford, CT, and the lower Connecticut River Valley. With the introduction of appropriate EMI modifications, the ROSCAM flies routinely over the Westover Air Force Base, with no apparent EMI.

Both color and black and white PC images obtained by the ROSCAM camera, when observing the roof scenario from the Millitech Tower, are shown in Figure 14. The lack of EMI is clearly evident. The details of the roof, including the construction line pattern are easily seen, along with the roof corner, the roof edge line, and the air conditioning unit located to the far left. The tall pine tree and its shadow are of course a main event.

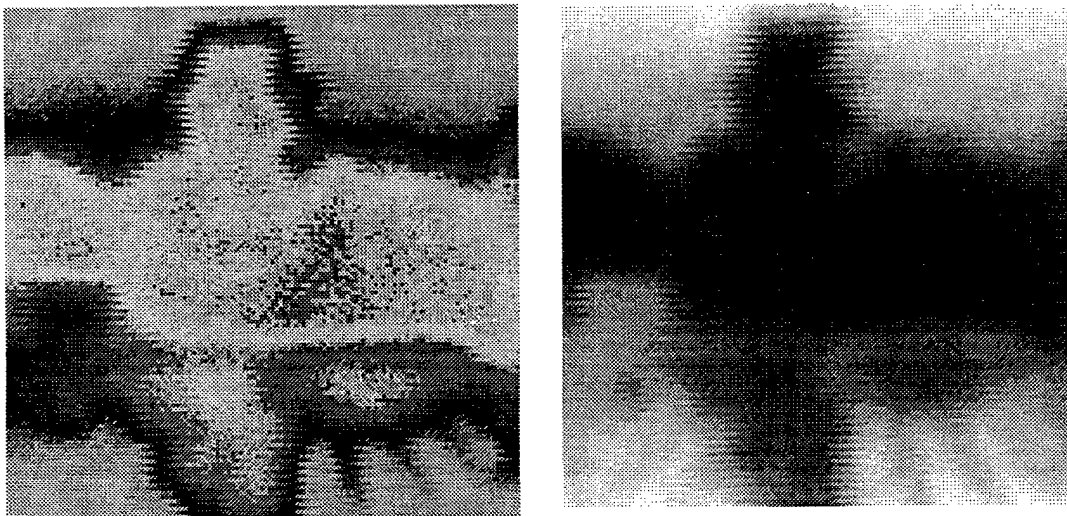


Figure 14. Passive Image from the Millitech Tower, ROSCAM A14B

V. CONCLUSIONS AND RECOMMENDATIONS

Based on the results of the performed measurements, the radarometer concept was verified in a laboratory environment.

A radiometer and radar were operated simultaneously on a non-interfering basis when using a common antenna. The output of the common antenna system was fed via a diplexer to the radar and radiometer channels. Verification of simultaneous operation, without interference in the performance of the radiometer by the radar, was demonstrated by recording the response of the

radiometer to a modulated noise input signal, when the radar was turned On and then Off. No difference in radiometer performance was noted between the On and Off conditions of the radar nor was a difference detected during either the CW or modulated transmitted signals were used (Test Setup #1). Demonstration of simultaneous active and passive imaging in the radarometer mode was also accomplished while imaging from the Millitech Tower (Test Setup #2).

Future investigation will focus on determining the nature of any limitations, or performance restraints, that may be imposed on the radarometer mode by an operational environment, particularly an airborne environment.

REFERENCES

1. C. Koh, "*Millimeter Wave Radar AGL Sensor Final Report*," Millitech Corporation, March 1997.

DISTRIBUTION LIST

AFRL-MN-EG-TR-2000-7006

DEFENSE TECHNICAL INFORMATION CENTER
ATTN: DTIC-OCA (ACQUISITION)
8725 JOHN J. KINGMAN ROAD, SUITE 0944
FT. BELVOIR VA 22060-6218

NAVAL AIR WEAPONS CENTER
ATTN: DR. DAVE BURDICK
CODE 472E00D
CHINA LAKE CA 93555-6001

COMDR, U.S. ARMY AVIATION AND MISSILE COMMAND
ATTN: AMSMI-RD-GC-N (MR. MONTE HELTON)
REDSTONE ARSENAL AL 35898-5241

IIT RESEARCH INSTITUTE/GACIAC
10 WEST 35TH STREET
CHICAGO IL 60616-3799

AIR UNIVERSITY LIBRARY
600 CHENNAULT CIRCLE, BLDG 1405
MAXWELL AFB AL 36112-6424

EGLIN AFB OFFICES:

AFRL/MN/CA-N
AFRL/MNOC-1 (STINFO Office)
AFRL/MNG
AFRL/MNGG
AFRL/MNGI
AFRL/MNGN
AFRL/MNGS
AFRL/MNA
AFRL/MNM